Microscopic investigations of advanced thin films for photonics

S Boninelli[1,*], A Shakoor[2], K Welma[2], TF Krauss[2], L O'Faolain[2], R Lo Savio[3], S Portalupi[3], D Gerace[3], M Galli[3], P Cardile[1], G Bellocchi[1], G Franzò[1], M Miritello[1], F Iacona[1] and F Priolo[1]

[1] MATIS IMM CNR and Dipartimento di Fisica e Astronomia, Università di Catania, via Santa Sofia 64, 95121 Catania, Italy
[2] SUPA, School of Physics and Astronomy, University of St. Andrews, Fife KY16 9SS, St. Andrews, United Kingdom
[3] Dipartimento di Fisica, Università di Pavia, via Bassi 6, 27100 Pavia, Italy

E-mail: simona.boninelli@ct.infn.it

Abstract. We present the different approaches we recently followed to achieve intense room temperature photoluminescence (PL) from Si-based materials. On one side we obtained sub-bandgap PL from H-related defects induced by the H_2 plasma treatment of Si photonic crystal (PhC) nanocavities. We demonstrated that a strong and narrow PL emission can be obtained in the PhC nanocavities due to the formation of a damaged layer mainly consisting of nanometric platelets and bubbles. An overall 40000-fold enhancement of the PL signal, with respect to pure crystalline Si, has been achieved and moreover the signal can be tuned in a wide range by only changing the PhC parameters. On the other side, we focused our attention on the properties of SiO_2 and SiOC host matrices doped with Eu ions. C addition produces a strong enhancement of the Eu PL with respect to pure SiO_2 films. The chemical and structural characterization of these materials reveals an extensive Eu clustering in SiO_2-based films, while C addition induces a significant reduction of this phenomenon, enhancing the fraction of optically active Eu ions. These results can be applied for the realization of efficient Si-based light sources.

1. Introduction

The achievement of a cheap and efficient Si-based light source working at room temperature (RT) is currently the foremost objective in the field of photonics. The main performances required for this source are electrical pumping, high efficiency at room temperature, tunability, easy integration in highly compact Si microphotonic devices. The lack of an efficient Si-based light source is a result of the intrinsic inability of Si to efficiently emit light, due to its indirect bandgap. In the last decades, in our group many approaches have been followed to increase the photoluminescence (PL) efficiency of Si-based materials, such as the use of Si nanocrystals embedded in SiO_2 [1, 2], their doping with light emitting impurities,

* To whom any correspondence should be addressed.

such as Er ions [3] and, very recently, the realization of light emitting nanowires fabricated by a maskless etching technique [4].

Aim of this paper is to present an overview of the new strategies we have recently followed in our group in order to achieve intense light emission from Si-based materials.

The first approach consists of the engineering of optically active defects in crystalline Si, since it has been demonstrated in the literature that it represents a powerful method to improve the PL from this material [5, 6, 7]. Very recently the enhancement of the sub-bandgap PL via the Purcell effect in photonic crystal (PhC) cavities fabricated on bare silicon-on-insulator (SOI) has been demonstrated. The PL emission was attributed to point defects induced by the H implantation used for the production of SOI during the Smart Cut^{TM} process [8, 9]. In those papers the authors expressed their intention to implement a suitable H_2 plasma treatment to increase the amount of optically active defects in order to further enhance the PL emission from the Si based PhC nanocavity. The purpose of this study is twofold: on one side we realized an extensive transmission electron microscopy (TEM) investigation concerning the thermal evolution of H-induced platelets in crystalline Si and their correlation with the PL properties of bulk SOI materials, on the other side, once having optimized the light emission properties in plasma treated SOI, we tried to enhance the emission from these optically active defects by introducing them in the active region of a PhC nanocavity. We explain the PL activity of H_2 plasma treated PhC nanocavities in terms of the damage induced in these structures by the process.

The second approach we want to present here regards Eu doping of Si-based materials, which has been recognized as a powerful method to provide intense PL signals spanning a wide wavelength range [10, 11, 12]. Eu ions, owing to the coexistence of both divalent (Eu^{2+}) and trivalent (Eu^{3+}) oxidation states, act as emitting centers at different wavelengths. However, the low Eu solid solubility in SiO_2 represents an important limit for the practical applications of this rare earth [13, 14]. Indeed, the main challenge for Eu application is represented by the availability of alternative host matrices, whose synthesis and processing are compatible with Si technology, which are simultaneously capable to efficiently host high concentrations of optically active Eu ions.

Here, we will compare the performances of pure SiO_2 and of SiOC as host matrices for optically active Eu ions. It will be shown that in the case of SiO_2, although both Eu^{2+} and Eu^{3+} emissions can be obtained, the efficiency of the light emission remains quite far from requirements for technological applications due to the extensive formation of Eu-containing precipitates. On the other hand, it will be shown that a SiOC matrix, owing to its chemical and structural properties, is able to ensure an intense and stable light emission centered at about 440 nm from Eu^{2+} ions, which could be of great interest for photonic applications.

2. Results and Discussion

2.1. H plasma treated SOI

For H plasma treatments, SOI films have been introduced in a parallel plate ion etching set-up where the power was fixed at 40 W and the treatment duration was 30 min. The chamber pressure was kept at 0.1 mbar and all treatments were carried at RT. In order to maximize the PL emission, the H plasma as-treated SOI samples were cut into small pieces and were subjected to thermal annealing in a conventional furnace under a controlled forming gas (FG) atmosphere at different temperatures ranging from 300 °C to 500 °C for 30 min.

The PL was measured in a confocal μPL setup where a 640 nm cw laser was focused onto the sample with a high numerical aperture objective (NA=0.8). The emitted light from the sample was collected by the same objective and filtered by a pin-hole. The filtered light was then fed into a grating spectrometer with an InGaAs detector. Further details on the experimental apparatus can be found in references [8,15].

To observe the damage induced by H plasma on bare SOI, we performed cross-sectional TEM measurements by using a JEOL JEM 2010 instrument operating at an acceleration voltage of 200 kV. All TEM samples have been prepared using standard mechanical grinding and argon ion milling with an incidence angle of 7° and the accelerating voltage set at 5 kV.

For cavity experiments, we used modified L3 PhC cavities, which are known to have very high Q/V values [16]. The cavity was designed to have a fundamental mode at 1550 nm with a lattice constant a = 420 nm and an $r/\mathbf{a}$ ratio of 0.28. The far-field mode was optimised by enlarging alternating holes around the cavity by 15 nm, thus forming a second order grating. This folds back the $\boldsymbol{k}$-vector components near the edge of the Brillouin zone, outside the light emission cone, into the centre, resulting in an increase of the vertical emission efficiency [17, 18].

In Fig. 1a, the cross-section of TEM image of the H plasma treated SOI is reported. All the TEM images have been acquired in off Bragg defocused bright field (BF) conditions in order to avoid the background strain contrast around each defect and to emphasise the Fresnel contrast between the edge of the defect itself and the surrounding crystalline Si matrix [19, 20]. We observe that the damaged region, extending about 40 nm below the surface, presents different kind of defects: in the first 10 nm the damage consists of bubbles with a mean diameter of a few nm while, going further in depth, a buried band of platelets is found. The thickness of the band is 30 nm, the mean diameter of platelets lying on (001) is 15 nm while the mean diameter of platelets lying on {111} is 10 nm. Energy filtered TEM (not shown) reveals that the 7 nm thick amorphous layer found on the top Si surface of the H_2 plasma treated sample consists of a SiO_2 film, probably due to the hydrogenation treatment, as already speculated by Ghica et al. [21]. Moreover, we studied the thermal evolution of H-induced defects by performing annealing in FG in the temperature range 300–500 °C for 30 min in order to better passivate dangling bonds and, consequently, to decrease the efficiency of the non•radiative processes. In Fig. 1b the TEM micrograph of the sample annealed at 350 °C is reported. The thickness of the damaged layer is slightly reduced to about 30 nm with respect the as-treated sample, while the width of the band of nanobubbles is still 10 nm. The drastic reduction of the damaged layer is due to a shrinking of the platelets band to about 10 nm. Indeed, the mean diameter of {111} platelets is reduced to 5-7 nm while the (001) platelets are completely dissolved. Finally, after a thermal treatment at 500 °C for 30 min, we observe in the TEM image reported in fig. 1c a strong reduction of the damage depth at less than 15 nm and defects consisting only of nanobubbles, because both the (001) and {111} platelets are completely dissolved.

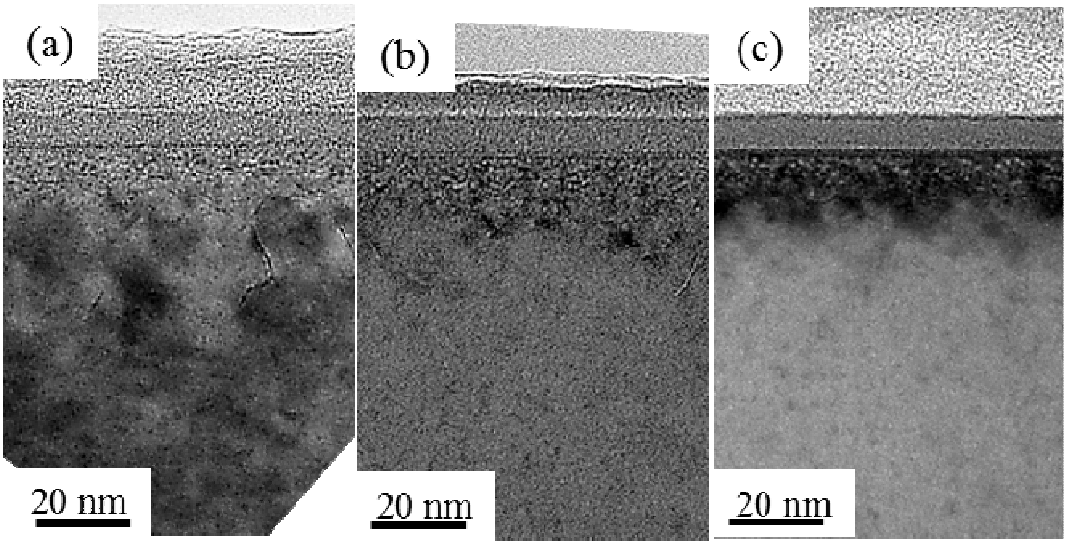

Figure 1. Defocused off-Bragg cross sectional TEM images of the H plasma treated SOI (a), after thermal annealing at 350 °C for 30 min (b) and at 500 °C for 30 min (c).

In order to correlate the structural properties with the optical ones, we have performed RT PL measurements on the H plasma treated SOI. In Fig. 2, the PL spectra of as-treated SOI (blue line and squares), of the SOI annealed at 350 °C (red line and circles) and at 500 °C (green line and triangles) are reported. The PL spectrum of the as-treated samples consists of a narrow band at ~1150 nm and a broad band with two main peaks at ~1300 nm and at ~1500 nm, in agreement with results reported in the literature [22]. After annealing at 350 °C for 30 min in FG ambient, we note an enhancement of PL with respect to the as-treated sample, while an almost full quenching is observed after the annealing at 500 °C for 30 min. These results, compared with the corresponding TEM analyses, put clearly in evidence the strong correlation between the PL intensity and the concentration of H-induced defects; indeed we note the highest PL signal in the sample annealed at 350 °C where the concentration of defects is still high and, conversely, a complete PL quenching has been observed in correspondence of the samples where there is only a residual trace of defects.

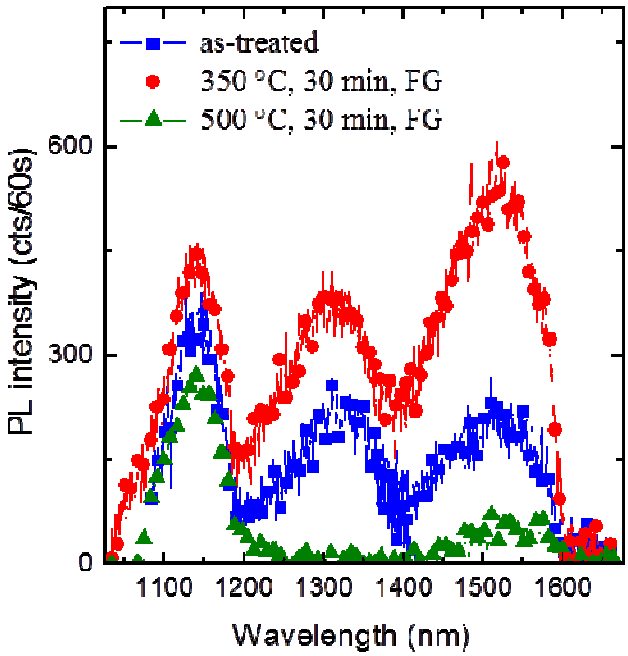

Figure 2. Room temperature PL spectra of H plasma treated SOI (blue squares), after thermal annealing at 350 °C for 30 min (red circles) and 500 °C for 30 min (green triangles).

An intense debate concerning the relationship between the broad PL band observed in H enriched samples and the H-induced damage is reported in the literature. Johnson and coworkers ascribe the PL emission observed in H plasma treated Si to the formation of the damage induced by the plasma treatment [23]. Moreover, a "strain-induced quantum-confined" model assumes the electron-hole recombination mechanism is allowed by the compressive strain in the platelets. The use of H to induce the damage further enhances the PL efficiency owing to its passivant role of non-radiative and other competitive radiative channels [22, 24].

Having optimized the light emission of H plasma•treated SOI, we have tried to enhance the emission from these optically active defects by introducing them in the active region of a L3 PhC nanocavity [25]. The scanning electron microscopy image of the cavity is shown in Fig. 3. The L3 PhC cavity was planned to have a fundamental mode at ~1.5 μm with a lattice constant a = 420 nm and an r/a ratio of 0.28, being r the radius of the PhC holes. The two holes adjacent to the cavity were reduced in size and displaced laterally to increase the cavity quality factor, Q.

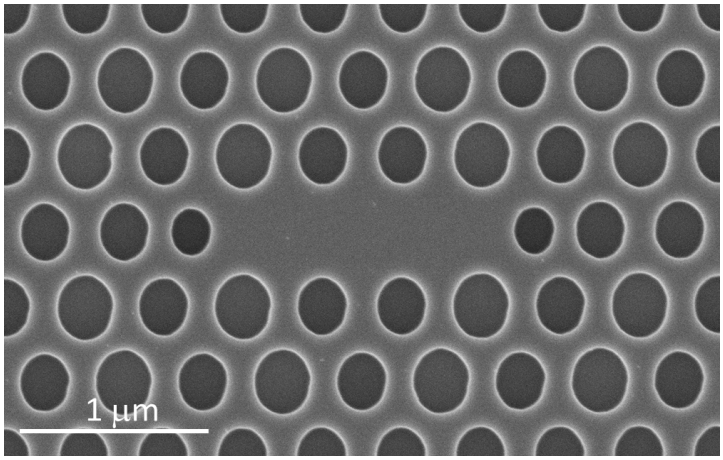

Figure 3. Scanning electron micrograph of L3 cavity

In order to control the fundamental cavity mode in the range 1300 – 1600 nm, we have also realized different PhC cavities having the period spanning from 370 to 450 nm. Indeed, in the H plasma-treated cavities, a strong and narrow PL emission can be obtained as demonstrated in Fig. 4. The sharp PL peaks, shown with different colours, correspond to the fundamental mode of each PhC cavity and can be tuned in a wide range of wavelengths by only changing the PhC parameters. We observe an overall 40000-fold increase of the PL signal at RT relative to bulk silicon.

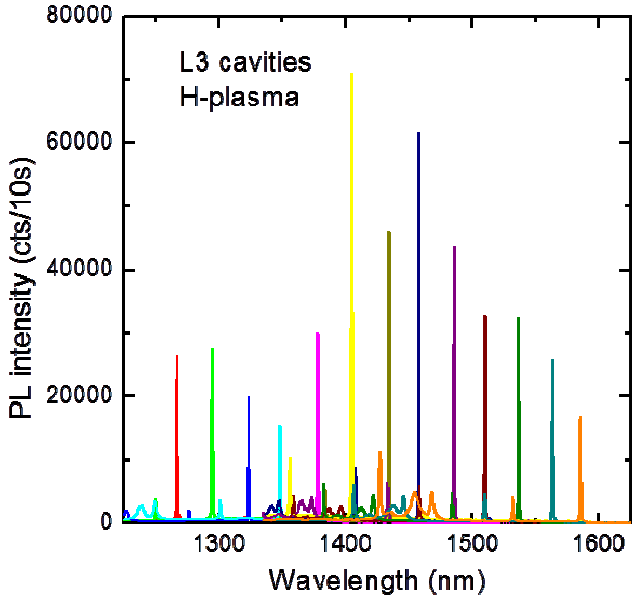

Figure 4. Room temperature PL spectra from H treated PhC cavities showing several peaks corresponding to the fundamental mode of cavities with different lattice periods.

2.2. Eu-doped SiO_2 and SiOC films

Eu-doped SiO_2 thin films were grown on (100) Si substrates heated at 400 °C by using an ultrahigh vacuum magnetron sputtering system. The base pressure was about 1×10^{-9} mbar. The deposition has been obtained by RF co-sputtering of 4 inches diameter, water-cooled SiO_2 and Eu_2O_3 targets (99.9% purity or higher). The deposition was carried out with a sputter upwards configuration in a 5×10^{-3} mbar Ar atmosphere. Sputter rates have been set in order to obtain Eu concentrations equal to 1.5 and 5.0×10^{20} cm^{-3}. Eu-doped SiOC thin films were grown by RF co-sputtering of SiO_2, SiC and Eu_2O_3 targets (99.9% purity or higher). Sputter rates have been set in order to obtain a C concentration of about 5 at.% and an Eu concentration of 1.5×10^{20} cm^{-3}. Both SiO_2- and SiOC-based films are about 200 nm thick. After deposition, samples were thermally treated for 1 h in ultra-pure N_2 ambient by using a horizontal furnace operating at temperatures ranging from 750 to 1000 °C.

A 200 kV JEOL 2010F microscope, equipped with a Gatan Image Filter, was used to investigate the chemical composition of films by the use of energy filtered TEM (EFTEM). PL measurements were performed by pumping with the 325 nm line of a He-Cd laser. The pump power was about 3 mW and the laser beam was chopped through an acousto-optic modulator at a frequency of 55 Hz. The PL signal was analyzed by a single grating monochromator and detected with a Hamamatsu visible light photomultiplier. Spectra were recorded with a lock-in amplifier using the acousto-optic modulator frequency as a reference. All the spectra have been measured at RT and corrected for the spectral system response.

In Fig. 5a the BF cross-sectional TEM image of a SiO_2 sample doped with 5.0×10^{20} Eu/cm^3 and annealed at 750 °C in N_2 ambient is displayed. The micrograph shows that no Eu precipitation occurs in the sample. If we increase the annealing temperature the formation of clusters occurs, as clearly visible in the BFTEM images reported in Fig. 5b (sample annealed at 900 °C in N_2) and in Fig. 5c (sample annealed at 1000 °C in N_2). At 900 °C clusters are almost homogeneously distributed throughout the film but their size markedly decreases on going from the interface with the substrate (where diameters as large as about 15 nm are found) towards the surface (where the mean diameter is a few nm). At 1000 °C most of the precipitates are found close to the surface and a marked increase of their maximum diameter (about 30 nm) occurs.

The EFTEM map of elemental Eu (not shown), obtained by energy filtering at 133 eV (corresponding to the N_{IV} edge of Eu) and by using the 3-windows method [26] demonstrates that all clusters contain Eu. Moreover, the diffraction pattern reported in the inset of Fig. 5c indicates that the Eu-containing precipitates are amorphous; the only crystalline clusters are detected at the interface with the Si substrate, as shown by the high resolution TEM image shown in the inset in Fig. 5b, referring to the cluster circled by the white line. The analysis of the corresponding Fast Fourier transform (not shown) reveals that these precipitates grow epitaxially with respect to the Si substrate and that these clusters have the crystalline structure of pure Eu_2O_3. The experimental evidence on the nature of the interfacial clusters, coupled with the well-known tendency of rare earth ions, including Eu and Er, to precipitate as an oxidized phase when they are embedded in SiO_2, allow us to reasonably conclude that also the amorphous precipitates consist of Eu oxides (and/or silicates).

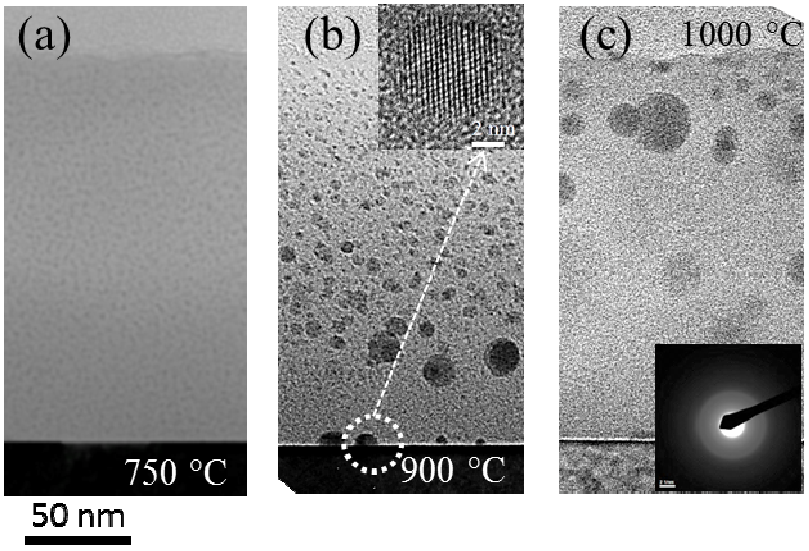

Figure 5. BF cross-sectionaol TEM images of the Eu-doped SiO_2 film annealed at 750 °C (a), at 900 °C (b) and at 1000 °C (c), for 1h in N_2 ambient. HR TEM image of the precipitate circled in white is shown in the inset of (b). The diffraction pattern of the Eu-doped SiO_2 film after the annealing at 1000 °C is reported in the inset of (c).

It is well known that Eu clustering is due to the low solid solubility of Eu in the SiO_2 matrix [12, 13, 27]. On the other hand, the peculiar temperature dependence of the precipitation phenomenon and the tendency of the clusters to move towards the surface when the annealing temperature is increased are certainly less expected. In the as-deposited sample the Eu ions are homogeneously distributed throughout the film; during the thermal process they acquire mobility but, in the absence of any concentration gradient, no relevant diffusion process is expected. Recently, we have demonstrated that the mobility acquired by the Eu atoms during the thermal annealing is due to the fact that the host matrix is O deficient and the Eu atoms, in order to be fully O-coordinated, diffuse towards the surface to trap O atoms from the contamination unavoidably present in a conventional furnace [28].

We have performed PL measurements to correlate the structural and the optical properties of Eu-doped SiO_2 films. Fig. 6 shows the PL spectra of as-deposited and annealed films, obtained at RT by exciting the samples with the 325 nm line of a He-Cd laser. The PL spectrum of the as-deposited sample consists of a broad band having its maximum at about 435 nm, corresponding to the emission of Eu^{2+} ions [29, 30], and of some narrow lines corresponding to the emission of Eu^{3+} ions [30]. After annealing the samples in N_2 ambient, we notice an increased intensity of the peak associated with Eu^{2+}, coupled with a shift to 450 nm (at 750 °C) and to 475 nm (at 900 °C); a further increase of the PL intensity and a small redshift are found at 1000 °C (spectrum not shown). The Eu^{3+} emission remains clearly visible as a peak at 750 °C and as a shoulder of the Eu^{2+} peak at 900 °C. The increased PL intensity in annealed samples accounts for a reduced density in the host matrix of defects which can constitute preferential channels for non-radiative de-excitation and for a better Eu coordination, while the peak redshift is related to the formation of regions characterized by different local Eu concentrations.

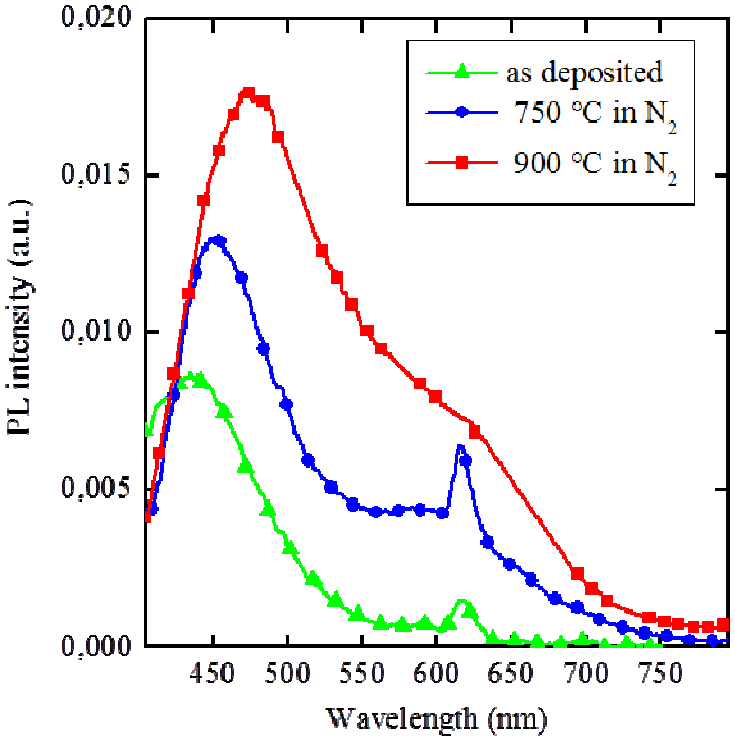

Figure 6. Room temperature PL spectra of Eu-doped SiO_2 films as-deposited and annealed at 750 and 900 °C, for 1h in N_2 ambient.

The cluster formation observed after thermal annealing, caused by the low solid solubility of Eu in silica, seriously limits the perspective of Eu application in photonics. Indeed, it is well established that the clustering occurring at high Eu concentration makes the rare-earth ions optically inactive. In this context a strong effort in the literature has been made to find strategies limiting the rare earth precipitation phenomenon [11, 12, 14, 27].

We have developed a new approach to make SiO_2 a better host for Eu ions. Indeed, it has been widely reported in literature that the Eu solubility can be remarkably increased by properly modifying the host matrix [31, 32]. We added to the Eu-doped SiO_2 matrix a C content of about 5 at. % in order to move from pure SiO_2 to a SiOC matrix, where the Eu concentration was set to 1.5×10^{20} cm^{-3}. Moreover, we deposited a SiO_2 capping layer (200 nm thick) on Eu-doped films before the annealing step, in order to avoid as much as possible additional Eu-O interactions and prevent the clustering formation. In Fig. 7, we compare the BF cross-sectional TEM images of Eu-doped SiO_2 (Figs. 7a) and SiOC films (Figs. 7b), capped with the SiO_2 film before the annealing at 900 °C in N_2 ambient. It is evident that C addition dramatically changes the structural properties of the Eu-doped SiO_2 films.

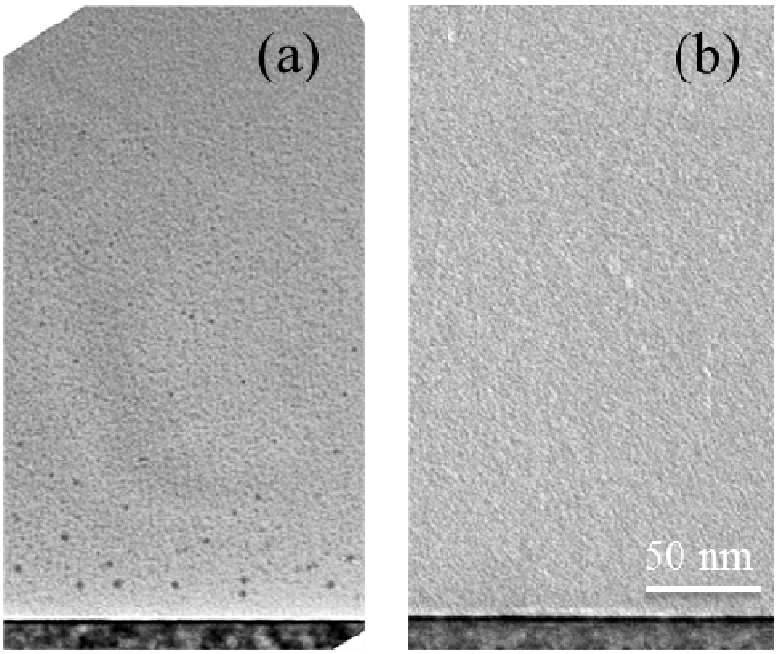

Figure 7. Cross-sectional TEM images of Eu-doped SiO_2 (a) and SiOC (b) annealed in N_2 ambient at 900 °C after the deposition of a SiO_2 capping layer.

Indeed, it is possible to note in Fig. 7a that, in the case of the SiO_2 matrix, a residual Eu clustering phenomenon is still observed in a region close to the interface with the Si substrate, while the Eu precipitation in a SiOC matrix is completely suppressed, as clearly shown by Fig. 7b. Fig. 8 reports the comparison between the RT PL spectrum of an Eu-doped SiOC sample annealed at 900 °C in N_2 (green line and triangles) and that of a SiO_2 sample containing the same Eu content and annealed under the same conditions (shown in Fig. 8 multiplied by a factor of 100 - blue line and squares). A very strong enhancement of the room temperature PL emission of about a factor of 250 has been obtained; furthermore, the peak is sharper and its maximum, detected at about 435 nm, is blue-shifted by about 60 nm. Fig. 8 also reports the PL spectra of Eu-doped SiOC samples annealed at 900 °C (red circles and line) after the SiO_2 cap deposition. In agreement with the capability of the capping layer to fully prevent Eu precipitation, demonstrated by the TEM image in Fig. 7b, a further enhancement of the PL intensity, accounting for about a factor of 1.5, has been obtained.

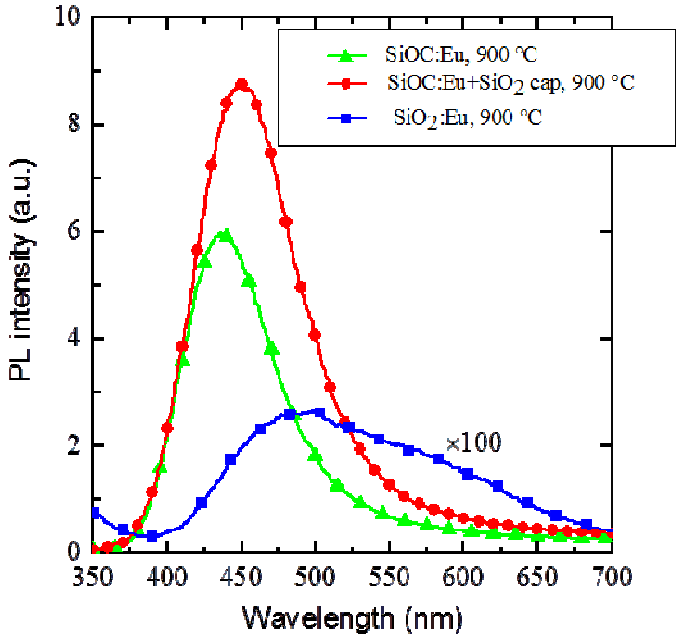

Figure 8. Room temperature PL spectra of Eu-doped SiOC and SiO_2 films annealed at 900 and in N_2 ambient. In the case of SiOC, spectra of both SiO_2-capped and uncapped samples are shown.

3. Conclusions

In this paper, we have reviewed the different approaches we recently followed for the realization and characterization of Si-based materials to be employed as efficient light emitters in Si photonics. The engineering of H-induced defects has been exploited in order to obtain light emission from crystalline Si. By comparing the structural and optical properties we clearly demonstrate that the luminescence is strictly correlated with the damage produced by the treatment, in agreement with the "strain-induced quantum-confined" model proposed in the literature. Moreover, an overall 40000−fold improvement of the emission from these optically active defects with respect to pure Si has been obtained by placing them in the active region of a PhC nanocavity. In addition, we demonstrated that the emission can be tuned over a wide range of wavelengths by only changing the PhC parameters.

On the other side, limits and perspectives of pure SiO_2 and SiOC matrices as a host for optically active Eu ions have been presented and discussed. In the case of SiO_2 the occurrence of an extensive Eu precipitation in thermally annealed films seems to be unavoidable. We have therefore proposed the addition of C to the Eu-doped SiO_2 matrix and a capping with SiO_2 as a strategy to minimize clustering phenomena and to improve the efficiency of RT light emission. Indeed, TEM data have demonstrated that Eu ions in SiOC are characterized by an enhanced mobility and solubility. This peculiarity leads to a strongly reduced Eu precipitation, and, as a consequence, to a very intense and stable light emission, centered at about 440 nm, from Eu^{2+} ions. Since SiOC can be considered a material fully compatible with Si technology and an appreciable electrical conduction is expected in this matrix, we believe that the Eu-doped SiOC films may open new and interesting perspectives for photonic applications of Eu-containing materials.

References

[1] Iacona F et al 2004 *J. Appl. Phys*. **95** 3723-3732.
[2] Boninelli S et al 2005 *Nanotechnology* **16** 3012–3016
[3] Franzò G et al 2003 *Appl. Phys. Lett*. **82** 3871-3873
[4] Irrera A et al 2012 *Nanotechnology* **23** 075204
[5] Henry A et al 1991 *J. Appl. Phys*. **70** 5597–5603
[6] Weber J 1991 *Phys. B, Cond. Mat*. **170** 201–217
[7] Canham L T et al 1989 *Mat. Sci. Eng. B* **4** 41–45
[8] Lo Savio et al 2011 *Appl. Phys. Lett.* **98** 201106
[9] Shakoor A et al 2012 *Phys. B* **407** 4027–4031
[10] Li D et al 2010 *Opt. Express* 18 27191-27196
[11] Rebohle L et al 2008 *Appl. Phys. Lett*. **93** 071908
[12] Rebohle L et al 2009 *J. Appl. Phys.* **106** 123103
[13] Afify N D et al 2009 *Phys. Rev. B* **79** 024202
[14] Lægsgaard J et al 2002 *Phys. Rev. B* 65, 174114
[15] Galli M et al 2009 *Appl. Phys. Lett*. **94** 071101
[16] Akahane Y et al 2003 *Nature* **425** 944-947
[17] Tran N V Q et al 2009 *Phys. Rev. B* **79** 041101
[18] Portalupi S L et al 2010 *Opt. Express* **18** 16064
[19] Grisolia J et al 2000 *Appl. Phys. Lett*. **76** 852-854
[20] Boninelli S et al 2006 *Appl. Phys. Lett*. **89** 171916
[21] Ghica C et al 2011 *J. Phys. D : Appl. Phys*. **44** 295401
[22] Weman H et al 1990 *J. Appl. Phys*. **87** 1013-1021
[23] Johnson N M et al 1987 *Phys. Rev. B* **35** 4166-4169
[24] Weman H et al 1990 *Phys. Rev. B* **42** 3109-3112
[25] Shakoor A et al 2012 *Laser Photonics Rev.* **7** 1 114
[26] Krivanek O L et al 1994 *Mater. Res. Soc. Symp. Proc*. **332** 341
[27] Nazarov A N et al 2010 *J. Appl. Phys*. **107** 123112
[28] Boninelli S et al 2013 *J. Appl. Phys* **113** 143503
[29] Tian Y et al 2011 *J. Appl. Phys.* **109** 053511
[30] Ye X et al 2009 *J. Appl. Phys.* **105** 064302
[31] G Bellocchi et al 2012 *Opt. Express* **20** 5501
[32] Q Zhang et al 2010 *Opt. Mater.* **32** 427